



Synthesis, characterization and *in vitro* anticancer activity of highly cytotoxic trithiolato diruthenium complexes of the type $[(\eta^6\text{-}p\text{-MeC}_6\text{H}_4\text{ }^i\text{Pr})_2\text{Ru}_2(\mu_2\text{-SR}^1)_2(\mu_2\text{-SR}^2)]^+$ containing different thiolato bridges

Federico Giannini^a, Julien Furrer^{a,**}, Georg Süss-Fink^{b,*}, Catherine M. Clavel^c, Paul J. Dyson^c

^a Department für Chemie und Biochemie, Universität Bern, CH-3012 Bern, Switzerland

^b Institut de Chimie, Université de Neuchâtel, CH-2000 Neuchâtel, Switzerland

^c Institut des Sciences et Ingénierie Chimiques, Ecole Polytechnique Fédérale de Lausanne (EPFL), CH-1015 Lausanne, Switzerland

ARTICLE INFO

Article history:

Received 31 January 2013

Received in revised form

22 April 2013

Accepted 28 April 2013

Keywords:

Arene ruthenium compounds

Dinuclear complexes

Thiolato complexes

Anticancer compounds

ABSTRACT

A series of cationic dinuclear *p*-cymene ruthenium complexes containing three thiolato bridges with different substituents at the sulfur atoms, $[(\eta^6\text{-}p\text{-MeC}_6\text{H}_4\text{ }^i\text{Pr})_2\text{Ru}_2(\mu_2\text{-SR}^1)_2(\mu_2\text{-SR}^2)]^+$ ($\text{R}^1 = \text{CH}_2\text{Ph}$, $\text{R}^2 = \text{Ph}$: **4**; $\text{R}^1 = \text{CH}_2\text{Ph}$, $\text{R}^2 = p\text{-C}_6\text{H}_4\text{ }^i\text{Pr}$: **5**; $\text{R}^1 = \text{CH}_2\text{Ph}$, $\text{R}^2 = p\text{-C}_6\text{H}_4\text{ }^i\text{Bu}$: **6**; $\text{R}^1 = \text{CH}_2\text{Ph}$, $\text{R}^2 = p\text{-C}_6\text{H}_4\text{OH}$: **7**; $\text{R}^1 = \text{CH}_2\text{Ph}$, $\text{R}^2 = p\text{-C}_6\text{H}_4\text{Br}$: **8**; $\text{R}^1 = \text{CH}_2\text{Ph}$, $\text{R}^2 = p\text{-C}_6\text{H}_4\text{F}$: **9**; $\text{R}^1 = \text{CH}_2\text{CH}_2\text{Ph}$, $\text{R}^2 = \text{Ph}$: **10**; $\text{R}^1 = \text{CH}_2\text{CH}_2\text{Ph}$, $\text{R}^2 = p\text{-C}_6\text{H}_4\text{ }^i\text{Pr}$: **11**; $\text{R}^1 = \text{CH}_2\text{CH}_2\text{Ph}$, $\text{R}^2 = p\text{-C}_6\text{H}_4\text{ }^i\text{Bu}$: **12**; $\text{R}^1 = \text{CH}_2\text{CH}_2\text{Ph}$, $\text{R}^2 = p\text{-C}_6\text{H}_4\text{OH}$: **13**; $\text{R}^1 = \text{CH}_2\text{CH}_2\text{Ph}$, $\text{R}^2 = p\text{-C}_6\text{H}_4\text{Br}$: **14**; $\text{R}^1 = \text{CH}_2\text{CH}_2\text{Ph}$, $\text{R}^2 = p\text{-C}_6\text{H}_4\text{F}$: **15**; $\text{R}^1 = \text{CH}_2\text{C}_6\text{H}_4\text{-}p\text{-}^i\text{Bu}$, $\text{R}^2 = \text{Ph}$: **16**; $\text{R}^1 = \text{CH}_2\text{C}_6\text{H}_4\text{-}p\text{-}^i\text{Bu}$, $\text{R}^2 = p\text{-C}_6\text{H}_4\text{ }^i\text{Pr}$: **17**; $\text{R}^1 = \text{CH}_2\text{C}_6\text{H}_4\text{-}p\text{-}^i\text{Bu}$, $\text{R}^2 = p\text{-C}_6\text{H}_4\text{ }^i\text{Bu}$: **18**; $\text{R}^1 = \text{CH}_2\text{C}_6\text{H}_4\text{-}p\text{-}^i\text{Bu}$, $\text{R}^2 = p\text{-C}_6\text{H}_4\text{OH}$: **19**; $\text{R}^1 = \text{CH}_2\text{C}_6\text{H}_4\text{-}p\text{-}^i\text{Bu}$, $\text{R}^2 = p\text{-C}_6\text{H}_4\text{Br}$: **20**; $\text{R}^1 = \text{CH}_2\text{C}_6\text{H}_4\text{-}p\text{-}^i\text{Bu}$, $\text{R}^2 = p\text{-C}_6\text{H}_4\text{F}$: **21**), have been obtained from the reaction of the neutral dithiolato intermediates $[(\eta^6\text{-}p\text{-MeC}_6\text{H}_4\text{ }^i\text{Pr})_2\text{Ru}_2\text{Cl}_2(\mu_2\text{-SR}^1)_2]$ ($\text{R}^1 = \text{CH}_2\text{Ph}$: **1**; $\text{R}^1 = \text{CH}_2\text{CH}_2\text{Ph}$: **2**; $\text{R}^1 = \text{CH}_2\text{C}_6\text{H}_4\text{-}p\text{-}^i\text{Bu}$: **3**) with the corresponding thiophenol R^2SH . All cationic complexes have been isolated as their chloride salts and fully characterized by spectroscopic and analytical methods. All complexes are highly cytotoxic against human ovarian cancer cells, the IC_{50} values being in the submicromolar range. The highest activity is shown by complex **6** with IC_{50} values of 48 nM against the A2780 cell line and 42 nM against the cisplatin-resistant line A2780cisR. This family of cationic trithiolato complexes belongs to the most cytotoxic ruthenium compounds ever reported. The catalytic activity selected representatives for the oxidation of glutathione (GSH) to GSSG has been investigated by NMR spectroscopy.

© 2013 Elsevier B.V. All rights reserved.

1. Introduction

Cisplatin, $[\text{cis-PtCl}_2(\text{NH}_3)_2]$, has become the most widely used metal-based anticancer drug ever since its introduction in 1978. Cisplatin was shown to attack DNA in the cells, preferentially binding to N7 of guanine, which ultimately triggers apoptosis (programmed cells death) [1]. However, its use in cancer therapy is limited by two factors: the established general toxicity of platinum compounds and the development of resistance of some tumors after an initial treatment of cisplatin [2]. These limitations have motivated new studies on alternative anticancer drugs containing

other metals. Nowadays ruthenium complexes are among the most studied non-platinum metal drugs for new therapies [3]. Ruthenium forms strong complexes with numerous ligands [4], different oxidation states are accessible under physiological conditions [5], and it can potentially mimic iron in binding to important carrier proteins [6,7]. Ruthenium(III) complexes such as NAMI-A, with an imidazole ring coordinated to the ruthenium center, and KP1019 with two indazole heterocycles coordinated to the metal center, have already entered clinical trials [8]. Studies have shown that KP1019 is efficiently taken up into cancer cells, possibly via interaction with transferrin [9], where they appear to induce Fenton type redox processes and intracellular radicals, leading to apoptosis [10]. Ruthenium(II) compounds are also interesting for the development of new anticancer drugs, in particular arene ruthenium complexes, such as the so-called RAPTA compounds containing a 1,3,5-triaza-7-phosphaadamantane (pta) ligand, the best characterized of the series

* Corresponding author. Tel.: +41 (0) 32 718 2405; fax: +41 (0) 32 718 2511.

** Corresponding author. Tel.: +41 (0) 31 631 4383; fax: +41 (0) 31 631 4887.

E-mail addresses: julien.furrer@dc.unibe.ch (J. Furrer), georg.suess-fink@unine.ch (G. Süss-Fink), georg.suess-fink@ich.unine.ch (G. Süss-Fink).

being RAPTA-C $[(\eta^6\text{-}p\text{-MeC}_6\text{H}_4\text{ }^i\text{Pr})\text{RuCl}_2(\text{pta})]$. This compound has only moderate *in vitro* anticancer activity, but significant activity with regard to reducing the number and weight of solid metastases, although not affecting the primary tumor [11].

Most studies on arene ruthenium compounds are concerned with mononuclear complexes, although highly active dinuclear arene ruthenium complexes have been reported: the dinuclear arene ruthenium complexes $(p\text{-}^i\text{PrC}_6\text{H}_4\text{Me})\text{Ru}(O,O\text{-C}_6\text{H}_5\text{O}_2\text{N}(\text{CH}_2)_n\text{NC}_6\text{H}_5\text{O}_2\text{-}O,O)\text{Ru}(p\text{-}^i\text{PrC}_6\text{H}_4\text{Me})$ containing a pyridone-derived linker show relevant cytotoxic effects against various cancer cell lines [12,13]. Recently, we have developed a new family of cationic dinuclear arene ruthenium complexes of general formula $[(\eta^6\text{-}p\text{-MeC}_6\text{H}_4\text{ }^i\text{Pr})_2\text{Ru}_2(\mu_2\text{-SR})_3]^+$ (R being alkyl or aryl), in which the two ruthenium atoms are bridged by three thiophenolato ligands. The corresponding chloride salts are highly cytotoxic toward the human ovarian cancer cell line A2780 and its cisplatin-resistant mutant A2780cisR, the IC_{50} values being in the submicromolar range [14]. Incubation with biological targets such as nucleotides and aminoacids, monitored by NMR spectroscopy, revealed interactions only with cysteine and glutathione, causing their oxidation to cystine and oxidized glutathione (GSSG), respectively. The complex could be recovered intact after the oxidation, which prompted us to postulate a catalytic role of the ruthenium complex as mode of action in the cytotoxic activity [15]. Extension of the series of dinuclear trithiophenolato compounds of general formula $[(\eta^6\text{-}p\text{-MeC}_6\text{H}_4\text{ }^i\text{Pr})_2\text{Ru}_2(\mu_2\text{-S-}p\text{-C}_6\text{H}_4\text{-X})_3]\text{Cl}$, where X are various functional groups showed that the cytotoxicity of the complexes is clearly influenced by the lipophilicity and the Hammett's constants of the corresponding thiols, although a direct correlation between cytotoxicity, catalytic oxidation activity and redox potentials could not be established [16], which is perhaps not surprising based on the different levels of cellular uptake of the compounds.

Here we report the synthesis, the *in vitro* anticancer activity and the catalytic glutathione oxidation activity of a new series of eighteen dinuclear *p*-cymene ruthenium complexes of the general formula $[(\eta^6\text{-}p\text{-MeC}_6\text{H}_4\text{ }^i\text{Pr})_2\text{Ru}_2(\mu_2\text{-SR}^1)_2(\mu_2\text{-SR}^2)]^+$, where R¹ is an aliphatic substituent and R² an aromatic substituent.

2. Results and discussion

2.1. Synthesis and characterization

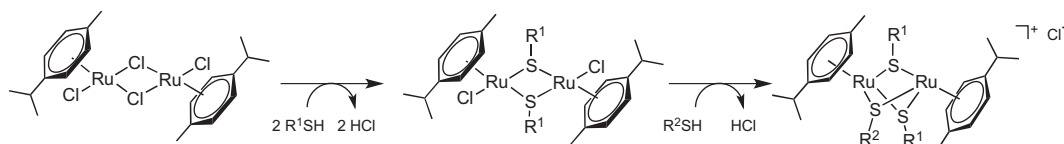
The neutral dichlorido dithiolato intermediates **1–3** are accessible from the reaction of the *p*-cymene–ruthenium dichloride dimer with 2 equivalents of phenylmethanethiol (for **1**), 2-phenylethanethiol (for **2**) and (4-*tert*-butylphenyl)methanethiol (for **3**) in ethanol at 0 °C, according to the published method [17]. These intermediates react in refluxing ethanol during 12–15 h with an excess (usually 6 equivalents) of the corresponding thiol to give the trithiolato complexes $[(\eta^6\text{-}p\text{-MeC}_6\text{H}_4\text{ }^i\text{Pr})_2\text{Ru}_2(\mu_2\text{-SR}^1)_2(\mu_2\text{-SR}^2)]^+$ (R¹ = CH₂Ph, R² = Ph: **4**; R¹ = CH₂Ph, R² = *p*-C₆H₄^{*i*}Pr: **5**; R¹ = CH₂Ph, R² = *p*-C₆H₄^{*t*}Bu: **6**; R¹ = CH₂Ph, R² = *p*-C₆H₄OH: **7**; R¹ = CH₂Ph, R² = *p*-C₆H₄Br: **8**; R¹ = CH₂Ph, R² = *p*-C₆H₄F: **9**; R¹ = CH₂CH₂Ph, R² = Ph: **10**; R¹ = CH₂CH₂Ph, R² = *p*-C₆H₄^{*i*}Pr: **11**; R¹ = CH₂CH₂Ph, R² = *p*-C₆H₄^{*t*}Bu: **12**; R¹ = CH₂CH₂Ph, R² = *p*-C₆H₄OH: **13**; R¹ = CH₂CH₂Ph, R² = *p*-C₆H₄Br: **14**; R¹ = CH₂CH₂Ph,

R² = *p*-C₆H₄F: **15**; R¹ = CH₂C₆H₄-*p*-^{*t*}Bu, R² = Ph: **16**; R¹ = CH₂C₆H₄-*p*-^{*t*}Bu, R² = *p*-C₆H₄^{*i*}Pr: **17**; R¹ = CH₂C₆H₄-*p*-^{*t*}Bu, R² = *p*-C₆H₄^{*t*}Bu: **18**; R¹ = CH₂C₆H₄-*p*-^{*t*}Bu, R² = *p*-C₆H₄OH: **19**; R¹ = CH₂C₆H₄-*p*-^{*t*}Bu, R² = *p*-C₆H₄Br: **20**; R¹ = CH₂C₆H₄-*p*-^{*t*}Bu, R² = *p*-C₆H₄F: **21**), which are isolated as orange to red air stable chloride salts in good to excellent yields, see Scheme 1. The analytical data are given in the Experimental section.

All compounds have been fully characterized by spectroscopic analytical methods, the ¹H and ¹³C NMR data providing a fingerprint for these complexes. For instance, the ¹H NMR spectrum of complex **4** (R¹ = CH₂Ph and R² = Ph) exhibits three multiplets in the aromatic region between 7.8 and 7.3 ppm, the first one at 7.78 ppm being attributed to the two *ortho* protons of the R² ligand and the second one at 7.33 ppm being assigned to the three remaining protons of the R² ligand. Interestingly, the ten aromatic protons of the two R¹ ligands appear as a single multiplet at 7.45 ppm. The two CH₂ benzyl groups show up as two singlets at 3.67 and 3.50 ppm, indicating that the two R¹ ligands are non-equivalent. As expected, their frequencies are slightly shifted low-field, because of the presence of the sulfur atom. The low-field shift of the signals of the aromatic protons of the *p*-cymene group is also characteristic for such complexes. In this case, the coordination to the ruthenium center causes a chemical shift of the four characteristic doublets to lower frequencies between 5.2 and 4.5 ppm with a coupling constant of 6 Hz, thus confirming that the two R¹ ligands are not equivalent. The two isopropyl groups of the *p*-cymene ligands give rise to a single septuplet at 1.9 ppm and to two doublets at 0.97 and 0.91 ppm for the two equivalent dimethyl groups. The two remaining methyl substituents of the two *p*-cymene ligands appear as a singlet at 1.76 ppm. The ¹H NMR spectrum of complex **10** (R¹ = CH₂CH₂Ph and R² = Ph) reveals nearly the same resonances as **4**, the first multiplet at 7.71 ppm being assigned to the two *ortho* protons of the R² substituent and the multiplet at 7.30 ppm being attributed to the three remaining protons of R². The ten aromatic protons of the two R¹ substituents appear as a single multiplet at 7.31 ppm. Typical for the complexes containing R¹ = CH₂CH₂Ph are four triplets in the region between 3.15 and 2.60 ppm, each with a coupling constant of 7.6 Hz, reflecting the four different CH₂ groups of the two R¹ substituents. In this case, the eight aromatic protons of the two *p*-cymene rings collapse into a single multiplet at 5.2 ppm. The ¹H NMR spectrum of complex **16** with R¹ = CH₂-*p*-C₆H₄^{*t*}Bu and R² = Ph is similar, the resonances of the aromatic protons of the R¹ ligands being displayed as two defined multiplets at 7.47 and 7.42 ppm, thus indicating the non-equivalence of the two groups. This is further confirmed by two distinct singlets at 1.37 and 1.33 ppm for the two *tert*-butyl protons and by two singlets at 3.62 and 3.44 ppm for the two benzyl CH₂ groups.

2.2. Cytotoxicity of **4–21**

The *in vitro* anticancer activity of the trithiolato complexes was evaluated against the human ovarian cancer cell line A2780 and the cisplatin-resistant mutant A2780cisR, using the MTT [3-(4,5-dimethylthiazol-2-yl)-2,5-diphenyltetrazoliumbromide] assay, which measures mitochondrial dehydrogenase activity as an indication of cell viability. The cytotoxicity of the complexes, expressed as IC_{50} values which represent the drug concentration required to



Scheme 1. Synthesis of complexes **4–21** as the chloride salts.

Table 1
Nanomolar cytotoxicities of complexes **4–21** toward A2780 and A2780cisR human ovarian cancer cells.

Complex	IC ₅₀ [nM] A2780	IC ₅₀ [nM] A2780cisR
4	128 ± 4	142 ± 6
5	72.0 ± 0.8	66.9 ± 2.2
6	47.8 ± 3	42.9 ± 1
7	134 ± 16.0	196 ± 11
8	172 ± 4	151 ± 9
9	124 ± 2.5	113.8 ± 0.3
10	120 ± 6	118.5 ± 3.4
11	57.8 ± 1.6	46.8 ± 0.3
12	74.4 ± 2.8	49.9 ± 1.9
13	298 ± 11	372 ± 13
14	125.5 ± 1.6	120.9 ± 3.5
15	141 ± 8	108 ± 7
16	55.5 ± 0.9	41.4 ± 0.7
17	153 ± 8	218 ± 14
18	163 ± 8	159.5 ± 1.3
19	132 ± 3.3	118.3 ± 2.1
20	97.3 ± 0.6	100.7 ± 1
21	139 ± 10	123 ± 4

cause 50% inhibition of cancer cell growth relative to control cells, are reported in Table 1.

All the complexes are highly cytotoxic against both cell lines with IC₅₀ values in the nanomolar range. Complex **6**, where R¹ = CH₂Ph and R² = C₆H₄^tBu, exhibits the highest cytotoxic effect against both cell lines, with IC₅₀ values of about 40 nM. These complexes are amongst the most active anticancer ruthenium compounds ever reported. To date, the most cytotoxic ruthenium complexes reported include dimeric complexes with pyridone-derived linkers [12,13], supramolecular arene ruthenium cages containing thiolato linkers [18], and dendritic systems terminated with arene ruthenium groups [19]. However, it should be noted that the supramolecular and dendrimer systems contain multiple ruthenium centers and per ruthenium the compounds reported herein are more cytotoxic.

The differences in cytotoxicity observed for these complexes can be related to the R¹ and R² ligands. In the series where R¹ = CH₂Ph, the aliphatic character as well as the lipophilicity of the substituent group in the *p*-position of the arene ligand gradually increases in going from R² = Ph (**4**), to *p*-C₆H₄ⁱPr (**5**) and *p*-C₆H₄^tBu (**6**), resulting in an enhanced cytotoxicity, see Table 2. Interestingly, the other complexes do not follow the same tendency, and for R¹ = CH₂C₆H₄^tBu the trend is even reversed. Thus, complex **16** (R² = Ph) exhibits the lowest IC₅₀ value, followed by

complex **17** (R² = C₆H₄ⁱPr) and then by complex **18** (R² = C₆H₄^tBu). For R¹ = CH₂CH₂Ph a relationship between the aliphatic nature of the R² substituent and the cytotoxicity is not apparent. Indeed, complexes **11** and **12** with R² = C₆H₄ⁱPr and C₆H₄^tBu, respectively, exhibit IC₅₀ values lower than complex **10** where R² = Ph. When the R² substituent contains a heteroatom such as O, Br or F, the nature of the R¹ ligand has practically no influence on the biological activity, these complexes showing almost the same cytotoxicity, except complex **13** with R¹ = CH₂CH₂Ph and R² = *p*-C₆H₄OH, which is by far the less cytotoxic of this series.

The subtle balance between hydrophobicity and lipophilicity of R¹ and R² for this family of complexes is consistent with the results we found for the series of trithiolato-bridged dinuclear ruthenium arene complexes containing three identical R groups. In this case, the cytotoxicity increases in the order H < Me < ⁱPr < ^tBu [16].

2.3. Correlations between cytotoxicity and Hammett's constants and lipophilicity

The Hammett constants (σ_p) related to the *para*-substituted phenyl rings of the R¹ and R² substituents reflect the electronic influence of the substituents [20] and the partition coefficients ($\log P$) of the thiols R¹SH and R²SH reflect the lipophilicity of the substituents. These calculated values are given in Table 2. For clarity, the complexes have been classified as a function of the R¹ substituent. As the trithiolato-bridged diruthenium core remains the same for all complexes, the lipophilicity of these complexes should vary only as a function of the R¹SH and R²SH $\log P$ parameters. The partition coefficients ($\log P$) were calculated using the ACD/ChemSketch software [21,22].

From Table 2, some interesting correlations between the Hammett constants (σ_p) of the *para*-aryl substituted groups of R¹ and R², the lipophilicity ($\log P$) of the thiol ligands and the IC₅₀ values for the A2780 and A2780cisR cell lines can be extracted. Taking the combined influences for the $\log P$ parameters for both R¹ and R² groups into account, it can be clearly seen that complexes with both ligands having $\log P$ coefficients inferior to 3.5 have IC₅₀ values higher than 100 nM. In contrast, if one of the two thiols has a $\log P$ value between 3.5 and 4.5, and the other one between 2.5 and 3.5, then the biological activity against both cellular lines is enhanced, presumably due to increased uptake as the more lipophilic compounds can more readily traverse cell membranes.

From the data shown in Table 2, we were also able to extract a relationship between the Hammett's constants of the substituents and the cytotoxicities. The complexes, in which one of the two R

Table 2
Comparison of cytotoxicities of **4–21** with physicochemical data for the thiols underlying the substituents R¹ and R². Calculated $\log P$ values are related to the thiols R¹SH and R²SH. Tabulated Hammett constants (σ_p) correspond to the *p*-C₆H₄X, where X is the substituent in *para* position of the phenyl ring of the R¹ and R² ligands.

Complex	R ¹	R ²	Log P (R ¹ SH)	σ_p -R ¹	Log P (R ² SH)	σ_p -R ²	IC ₅₀ [nM] A2780	IC ₅₀ [nM] A2780cisR
4	CH ₂ Ph	Ph	2.74	0.00	2.52	0.00	128	142
10	CH ₂ CH ₂ Ph	Ph	2.87	0.00	2.52	0.00	120	118.5
16	CH ₂ C ₆ H ₄ ^t Bu	Ph	4.43	-0.20	2.52	0.00	55.5	41.4
5	CH ₂ Ph	C ₆ H ₄ ⁱ Pr	2.74	0.00	3.86	-0.15	72	66.9
11	CH ₂ CH ₂ Ph	C ₆ H ₄ ⁱ Pr	2.87	0.00	3.86	-0.15	57.8	46.8
17	CH ₂ C ₆ H ₄ ^t Bu	C ₆ H ₄ ⁱ Pr	4.43	-0.20	3.86	-0.15	153	218
6	CH ₂ Ph	C ₆ H ₄ ^t Bu	2.74	0.00	4.21	-0.20	47.8	42.9
12	CH ₂ CH ₂ Ph	C ₆ H ₄ ^t Bu	2.87	0.00	4.21	-0.20	74.4	49.9
18	CH ₂ C ₆ H ₄ ^t Bu	C ₆ H ₄ ^t Bu	4.43	-0.20	4.21	-0.20	163	159.5
7	CH ₂ Ph	C ₆ H ₄ OH	2.74	0.00	1.68	-0.37	134	196
13	CH ₂ CH ₂ Ph	C ₆ H ₄ OH	2.87	0.00	1.68	-0.37	298	372
19	CH ₂ C ₆ H ₄ ^t Bu	C ₆ H ₄ OH	4.43	-0.20	1.68	-0.37	132	118.3
8	CH ₂ Ph	C ₆ H ₄ Br	2.74	0.00	3.53	0.23	172	151
14	CH ₂ CH ₂ Ph	C ₆ H ₄ Br	2.87	0.00	3.53	0.23	125.5	120.9
20	CH ₂ C ₆ H ₄ ^t Bu	C ₆ H ₄ Br	4.43	-0.20	3.53	0.23	97.3	100.7
9	CH ₂ Ph	C ₆ H ₄ F	2.74	0.00	2.81	0.06	124	113.8
15	CH ₂ CH ₂ Ph	C ₆ H ₄ F	2.87	0.00	2.81	0.06	141	108
21	CH ₂ C ₆ H ₄ ^t Bu	C ₆ H ₄ F	4.43	-0.20	2.81	0.06	139	123

groups (R^1 or R^2) has a σ_p value between 0 and -0.20 , while the other one has a $\sigma_p = 0.00$, display the best IC_{50} values of the series. All deviations from this optimal range of Hammett's constants lead to higher IC_{50} values.

Interestingly, the two optimal ranges for both the Hammett's constants and the $\log P$ parameters coincide for the best cytotoxicities. These results are in agreement with those obtained for our previous series of ruthenium compounds $[(\eta^6\text{-}p\text{-MeC}_6\text{H}_4\text{ }^i\text{Pr})_2\text{Ru}_2(\mu_2\text{-SR})_3]\text{Cl}$, the lowest IC_{50} values being obtained for complexes having $\log P$ coefficients between 3.0 and 4.2 for the A2780 cell line, and between 2.8 and 4.3 for the A2780cisR cell line, while the Hammett constants were in the range between -0.20 and 0.00 [16].

In contrast to our previously reported series of cationic dinuclear *p*-cymene ruthenium trithiophenolato complexes of the type $[(\eta^6\text{-}p\text{-MeC}_6\text{H}_4\text{ }^i\text{Pr})_2\text{Ru}_2(\mu_2\text{-SC}_6\text{H}_4\text{-}p\text{-X})_3]^+$, which showed large differences in the *in vitro* anticancer activity [16], all complexes of the present series $[(\eta^6\text{-}p\text{-MeC}_6\text{H}_4\text{ }^i\text{Pr})_2\text{Ru}_2(\mu_2\text{-SR}^1)_2(\mu_2\text{-SR}^2)]^+$ are highly cytotoxic against human ovarian cancer cells. Our previous results suggested that complexes possessing Hammett constants in the range $-0.2 < \sigma_p < 0$ and $\log P$ values above 3.0 have the lowest IC_{50} values, *i.e.* in the nanomolar region [16]. The cytotoxicities found for the present series, which are much less varied, can be explained by the fact that the physicochemical properties of the compounds can be easily fine-tuned, since complexes **4–21** have two different substituents R^1 and R^2 in the thiolato ligands. Thus, a less favorable substituent R^1 can be counterbalanced by a better substituent R^2 . As a result, the overall cytotoxic properties of all complexes are at least acceptable. Typical examples are complexes **9**, **15**, and **21** all containing a *p*- $\text{C}_6\text{H}_4\text{F}$ substituent with non-optimal physicochemical properties. Their IC_{50} values are still in the range 108–141 nM, thanks to the presence of a fluorine-free substituent in the other thiolato bridges, as compared to $[(\eta^6\text{-}p\text{-MeC}_6\text{H}_4\text{ }^i\text{Pr})_2\text{Ru}_2(\mu_2\text{-SC}_6\text{H}_4\text{-}p\text{-F})_3]^+$ which is much less cytotoxic ($IC_{50} = 660$ nM for A2780 and $IC_{50} = 1050$ nM for A2780cisR) [16].

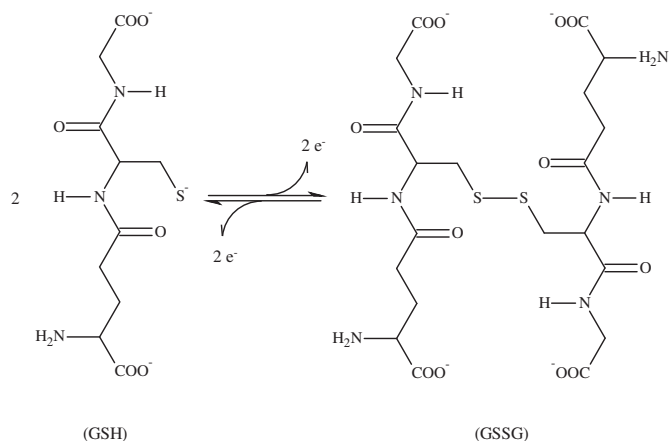
2.4. Catalytic oxidation of glutathione

The dinuclear arene ruthenium trithiolato cations are inert to substitution of both, arene ligands and thiolato bridges; therefore, the question of their mode of action in living cell arises. Since we had observed earlier that the complex $[(\eta^6\text{-}p\text{-MeC}_6\text{H}_4\text{ }^i\text{Pr})_2\text{Ru}_2(\mu_2\text{-SC}_6\text{H}_4\text{-}p\text{-Me})_3]^+$ catalyzes the oxidation of glutathione [16], it is reasonable to assume that this might be at least one of the reasons for the high cytotoxicity of this type of complexes.

The tripeptide glutathione (GSH) is found in all living cells with a concentration of approximately 5 mM. It is derived from the three aminoacids *L*-cysteine, *L*-glutamic acid and glycine. GSH represents the major endogenous antioxidant in living cells, preventing damage to important cellular components caused by reactive oxygen species such as free radicals and peroxides [23]. In healthy cells, more than 90% of the total glutathione pool is present in the reduced form (GSH) and less than 10% exist in the oxidized disulfide form (GSSG) [24,25].

Recently, we studied the interaction of GSH with a series of highly cytotoxic compounds of the general formula $[(\eta^6\text{-}p\text{-MeC}_6\text{H}_4\text{ }^i\text{Pr})_2\text{Ru}_2(\text{SR})_3]\text{Cl}$ (where R are *p*-substituted phenyl groups) and found them to catalyze the oxidation of glutathione to GSSG in water. However, a direct correlation between their cytotoxicity (IC_{50}) and their turnover frequency (TOF₅₀) for their catalytic activity of glutathione oxidation was not observed [16].

For this new series of complexes, we also studied the catalytic activity for the oxidation of GSH to GSSG (Scheme 2) by NMR spectroscopy. To evaluate the catalytic activity, we incubated the most (lowest IC_{50}) and the least (highest IC_{50}) cytotoxic complex of each of the three groups ($R^1 = \text{CH}_2\text{Ph}$, $\text{CH}_2\text{CH}_2\text{Ph}$ and $\text{CH}_2\text{C}_6\text{H}_4\text{-}$



Scheme 2. Oxidation of glutathione (GSH) to give GSSG.

p-^tBu) with GSH in a ratio 1:100, in a solution of $\text{D}_2\text{O}/\text{DMSO-d}_6$ (99:1), at pH 7 and 37 °C and in aerobic atmosphere (the GSH autoxidation in the presence of O_2 being less than 5% in 24 h).

As evidenced by the disappearance of the $\beta\text{-CH}_2$ resonances of GSH at $\delta \sim 3.0$ ppm and the simultaneous appearance of two new signals at $\delta \sim 3.1$ ppm and $\delta \sim 3.4$ ppm, the six experiments led to the complete oxidation of GSH to GSSG within 24 h. The TOF₅₀ values, which correspond to the turnover frequencies for each complex as catalyst at about 50% conversion of GSH to GSSG, are reported in Table 3, in comparison with the corresponding IC_{50} values.

A direct correlation of IC_{50} values with the TOF₅₀ values cannot be established. Indeed, the TOF₅₀ of the most cytotoxic complex **6** ($IC_{50} < 50$ nM for both cell lines) is only 4.59 h^{-1} , whereas it increases to 6.44 h^{-1} for the less cytotoxic complex **8** ($IC_{50} > 150$ nM for both cell lines) and goes to 7.23 h^{-1} for complex **11** which has a comparable biological activity as **6**. While there is not a direct correlation between catalytic oxidation of GSH and cytotoxicity, it is not unexpected as the uptake of the complexes into cancer cells depends on the $\log P$ values and therefore the amount of complex in the cells differs for each complex. Thus, although it remains to be proven that the mechanism of cell death is due to the catalytic oxidation of GSH, such a mechanism cannot be excluded, at least in part. Moreover, since the complexes show comparable cytotoxicities in both the A2780 and cisplatin resistant A2780R cell lines a mode of action different to that of cisplatin, *i.e.* primarily DNA binding, can be excluded to some extent.

3. Conclusion

To the best of our knowledge, the new diruthenium trithiolato complexes, all obtained in good to excellent yields, are among the most cytotoxic arene ruthenium compounds ever reported.

Table 3
Comparison of cytotoxicities (IC_{50}) with catalytic activity (TOF₅₀) of the most and the least cytotoxic complexes.

Complex	R^1	R^2	TOF ₅₀ (h^{-1})	IC_{50} [nM] A2780	IC_{50} [nM] A2780cisR
6	CH_2Ph	$\text{C}_6\text{H}_4\text{ }^t\text{Bu}$	4.59	47.8	42.9
8	CH_2Ph	$\text{C}_6\text{H}_4\text{Br}$	6.44	172	151
11	$\text{CH}_2\text{CH}_2\text{Ph}$	$\text{C}_6\text{H}_4\text{ }^i\text{Pr}$	7.23	57.8	46.8
13	$\text{CH}_2\text{CH}_2\text{Ph}$	$\text{C}_6\text{H}_4\text{OH}$	7.02	298	372
16	$\text{CH}_2\text{C}_6\text{H}_4\text{ }^t\text{Bu}$	Ph	5.64	55.5	41.4
18	$\text{CH}_2\text{C}_6\text{H}_4\text{ }^t\text{Bu}$	$\text{C}_6\text{H}_4\text{ }^t\text{Bu}$	6.40	163	159.5

Interestingly, all complexes show comparable effects on both, cisplatin-sensitive and cisplatin-resistant human ovarian cancer cells. It can be assumed that the catalytic oxidation of GSH to GSSG plays a role in the biological activity of these complexes, but other modes of action such as interactions with enzymes and/or DNA, may also be involved. The cytotoxicity does not appear to correlate to the catalytic oxidation, but this may be due to the fact that the catalytic oxidation was studied in NMR tubes, while the cytotoxicity was determined with cancer cells. Therefore, the catalytic GSH oxidation activity cannot be ruled out as mode of action of these highly cytotoxic complexes, since the cytotoxicity correlates well with lipophilicity, and hence uptake of the complexes into cancer cells is likely to differ significantly.

From the results obtained, we can confirm that the lipophilicity plays an important role for this kind of drugs, as also shown for other types of arene ruthenium compounds [26,27]. The optimal range of partition coefficients and Hammett's constants leading to the best IC₅₀ values follows the same tendency found previously. Overall, these results help to identify the structural features for increasing the *in vitro* anticancer activity, the cellular uptake and the selectivity for a particular biological target.

4. Experimental

4.1. Materials and methods

The starting material $[(\eta^6\text{-}p\text{-MeC}_6\text{H}_4\text{Pr})_2\text{Ru}_2\text{Cl}_4]$ and the three neutral dithiolato complexes $[(\eta^6\text{-}p\text{-MeC}_6\text{H}_4\text{Pr})_2\text{Ru}_2\text{Cl}_2(\mu_2\text{-S-CH}_2\text{Ph})_2]$ (**1**) $[(\eta^6\text{-}p\text{-MeC}_6\text{H}_4\text{Pr})_2\text{Ru}_2\text{Cl}_2(\mu_2\text{-S-CH}_2\text{CH}_2\text{Ph})_2]$ (**2**) and $[(\eta^6\text{-}p\text{-MeC}_6\text{H}_4\text{Pr})_2\text{Ru}_2\text{Cl}_2(\mu_2\text{-S-CH}_2\text{-}p\text{-C}_6\text{H}_4\text{Bu})_2]$ (**3**) were prepared according to published methods [16]. All other reagents were commercially available and were used without further purification.

NMR spectra were recorded with a Bruker 400 MHz spectrometer. Electrospray mass spectra were obtained in positive- or negative-ion mode with an LCQ Finnigan mass spectrometer. Microanalyses were performed by the Mikroelementaranalytisches Laboratorium, ETH Zürich (Switzerland).

4.2. Synthesis of complexes $[(\eta^6\text{-}p\text{-MeC}_6\text{H}_4\text{Pr})_2\text{Ru}_2(\mu_2\text{-SR}^1)_2(\mu_2\text{-SR}^2)]^+$ (**4–21**)

After dissolution of the neutral dithiolato complex **1** (80 mg, 0.101 mmol), **2** (80 mg, 0.098 mmol), **3** (80 mg, 0.089 mmol) in technical-grade EtOH (50 ml) under reflux, the corresponding thiol (6 equiv.; SR = SPh: 62.5 μ l, 60.4 μ l, 54.8 μ l; *S-p*-C₆H₄Pr: 94.7 μ l, 91.4 μ l, 83 μ l; *S-p*-C₆H₄Bu: 105 μ l, 101.4 μ l, 92 μ l; *S-p*-C₆H₄OH: 76.8 mg, 74.2 mg, 67.4 mg; *S-p*-C₆H₄Br: 115 mg, 111.2 mg, 101 mg; *S-p*-C₆H₄F: 64.9 μ l, 62.6 μ l, 56.9 μ l) was added to the hot solution, which was then refluxed for 15 h. After evaporation of the solvent, the residue was purified by column chromatography on silica gel with dichloromethane/ethanol (9:1) as eluent. The yellow to brownish products were isolated as chloride salts and dried under vacuum.

4.2.1. Data for **[4]Cl**

Yield: 76.6 mg (88%). C₄₀H₄₇ClRu₂S₃·½CH₂Cl₂ (904.05): calcd. C 53.81, H 5.35; found C 54.02, H 5.56. ESI MS (MeOH): *m/z* = 826.6 [M + H]⁺. ¹H NMR (400 MHz, CDCl₃): δ = 7.78 (m, 2H, SC₆H₅), 7.45 (m, 10H, CH₂C₆H₅), 7.33 (m, 3H, SC₆H₅), 5.16 (d, ³*J* = 6.0 Hz, 2H, *p*-MeC₆H₄ⁱPr), 5.05 (d, ³*J* = 6.0 Hz, 2H, *p*-MeC₆H₄ⁱPr), 4.88 (d, ³*J* = 6.0 Hz, 2H, *p*-MeC₆H₄ⁱPr), 4.71 (d, ³*J* = 6.0 Hz, 2H, *p*-MeC₆H₄ⁱPr), 3.67 (s, 2H, SCH₂), 3.50 (s, 2H, SCH₂) 1.9 [sept, ³*J* = 6.8 Hz, 2H, *p*-MeC₆H₄CH(CH₃)₂], 1.76 (s, 6H, *p*-CH₃C₆H₄ⁱPr), 0.97 [d, ³*J* = 6.8 Hz, 6H, *p*-MeC₆H₄CH(CH₃)₂], 0.91 [d, ³*J* = 6.8 Hz, 6H,

p-MeC₆H₄CH(CH₃)₂] ppm. ¹³C{¹H} NMR (100 MHz, CDCl₃): δ = 139.8, 139.7, 137.7, 132.7, 129.6, 129.4, 129, 128.8, 128.6, 128.5, 128.2, 128.1, 107.2, 100.1, 83.8, 82.4, 40.2, 39.9, 30.9, 23.2, 22.5, 18.1 ppm.

4.2.2. Data for **[5]Cl**

Yield: 79.4 mg (87%). C₄₃H₅₃ClRu₂S₃ (904.11): calcd. C 57.15, H 5.91; found C 57.44, H 6.02. ESI MS (MeOH + CH₂Cl₂ + CH₃CN): *m/z* = 868.6 [M]⁺. ¹H NMR (400 MHz, CDCl₃): δ = 7.61 (d, ³*J* = 8.4 Hz, 2H, *S-p*-C₆H₄ⁱPr), 7.42 (m, 10H, SCH₂C₆H₅), 7.12 (d, ³*J* = 8.4 Hz, 2, *S-p*-C₆H₄ⁱPr), 5.07 (d, ³*J* = 6.0 Hz, 2H, *p*-MeC₆H₄ⁱPr), 4.94 (d, ³*J* = 6.0 Hz, 2H, *p*-MeC₆H₄ⁱPr), 4.83 (d, ³*J* = 6.0 Hz, 2H, *p*-MeC₆H₄ⁱPr), 4.60 (d, ³*J* = 6.0 Hz, 2H, *p*-MeC₆H₄ⁱPr), 3.60 (s, 2H, SCH₂C₆H₅), 3.42 (s, 2H, SCH₂C₆H₅), 2.86 [sept, ³*J* = 6.8 Hz, 1H, *S-p*-C₆H₄CH(CH₃)₂], 1.81 [sept, ³*J* = 7.2 Hz, 2H, *p*-MeC₆H₄CH(CH₃)₂], 1.76 (s, 6H, *p*-CH₃C₆H₄ⁱPr), 1.22 [d, ³*J* = 6.8 Hz, 6H, *S-p*-C₆H₄CH(CH₃)₂], 0.92 [d, ³*J* = 7.2 Hz, 6H, *p*-MeC₆H₄CH(CH₃)₂], 0.86 [d, ³*J* = 7.2 Hz, 6H, *p*-MeC₆H₄CH(CH₃)₂] ppm. ¹³C{¹H} NMR (100 MHz, CDCl₃): δ = 147.7, 139.9, 139.8, 134.4, 132.6, 129.6, 129.4, 128.8, 128.7, 128.2, 128.0, 127.1, 106.7, 100.5, 84.6, 83.5, 83.4, 82.5, 40.3, 40.0, 33.8, 30.7, 23.9, 23.3, 22.4, 18.2 ppm.

4.2.3. Data for **[6]Cl**

Yield: 89.9 mg (97%). C₄₄H₅₅ClRu₂S₃·¾CH₂Cl₂ (981.4): calcd. C 54.77, H 5.80; found C 54.40, H 6.12. ESI MS (MeOH + CH₂Cl₂ + CH₃CN): *m/z* = 882.7 [M]⁺. ¹H NMR (400 MHz, CDCl₃): δ = 7.65 [d, ³*J* = 8.4 Hz, 2H, *S-p*-C₆H₄C(CH₃)₃], 7.43 (m, 10H, SCH₂C₆H₅), 7.30 [d, ³*J* = 8.4 Hz, 2H, *S-p*-C₆H₄C(CH₃)₃], 5.13 (d, ³*J* = 6.0 Hz, 2H, *p*-MeC₆H₄ⁱPr), 4.97 (d, ³*J* = 6.0 Hz, 2H, *p*-MeC₆H₄ⁱPr), 4.88 (d, ³*J* = 6.0 Hz, 2H, *p*-MeC₆H₄ⁱPr), 4.63 (d, ³*J* = 6.0 Hz, 2H, *p*-MeC₆H₄ⁱPr), 3.65 (s, 2H, SCH₂C₆H₅), 3.47 (s, 2H, SCH₂C₆H₅), 1.79 [sept, ³*J* = 6.8 Hz, 2H, *p*-MeC₆H₄CH(CH₃)₂], 1.77 (s, 6H, *p*-CH₃C₆H₄ⁱPr), 1.30 [s, 9H, *S-p*-C₆H₄C(CH₃)₃], 0.91 [d, ³*J* = 6.8 Hz, 6H, *p*-MeC₆H₄CH(CH₃)₂], 0.86 [d, ³*J* = 7.2 Hz, 6H, *p*-MeC₆H₄CH(CH₃)₂] ppm. ¹³C{¹H} NMR (100 MHz, CDCl₃): δ = 151.9, 139.9, 139.8, 134.2, 132.3, 129.6, 129.5, 128.8, 128.6, 128.2, 128.0, 125.9, 106.5, 100.6, 84.8, 83.4, 83.3, 82.6, 40.3, 40.1, 34.7, 31.2, 30.7, 23.4, 22.4, 18.2 ppm.

4.2.4. Data for **[7]Cl**

Yield: 75.3 mg (85%). C₄₀H₄₇ClORu₂S₃ (877.6): calcd. C 54.74, H 5.40; found C 54.55, H 5.70. ESI MS (MeOH + CH₂Cl₂): *m/z* = 842.3 [M]⁺. ¹H NMR (400 MHz, CDCl₃): δ = 10.31 (s, 1H, *S-p*-C₆H₄OH), 7.41 (m, 14H, SCH₂C₆H₅ + *S-p*-C₆H₄OH), 5.06 (d, ³*J* = 6.0 Hz, 2H, *p*-MeC₆H₄ⁱPr), 4.94 (d, ³*J* = 6.0 Hz, 2H, *p*-MeC₆H₄ⁱPr), 4.71 (m, 4H, *p*-MeC₆H₄ⁱPr), 3.62 (s, 2H, SCH₂C₆H₅), 3.45 (s, 2H, SCH₂C₆H₅), 2.04 [sept, ³*J* = 6.8 Hz, 2H, *p*-MeC₆H₄CH(CH₃)₂], 1.73 (s, 6H, *p*-CH₃C₆H₄ⁱPr), 1.05 [d, ³*J* = 6.8 Hz, 6H, *p*-MeC₆H₄CH(CH₃)₂], 0.99 [d, ³*J* = 6.8 Hz, 6H, *p*-MeC₆H₄CH(CH₃)₂] ppm. ¹³C{¹H} NMR (100 MHz, CDCl₃): δ = 159.9, 139.9, 139.7, 133.3, 129.5, 129.2, 128.8, 128.7, 128.2, 128.1, 124.0, 117.1, 107.5, 99.7, 84.1, 83.7, 83.2, 82.0, 39.9, 39.5, 31.0, 23.1, 22.7, 18.0 ppm.

4.2.5. Data for **[8]Cl**

Yield: 85.5 mg (90%). C₄₀H₄₆BrClRu₂S₃·½CH₂Cl₂·EtOH (1029): calcd. C 49.55, H 5.01; found C 49.85, H 5.16. ESI MS (MeOH): *m/z* = 904.8 [M]⁺. ¹H NMR (400 MHz, CDCl₃): δ = 7.72 (d, ³*J* = 8.4 Hz, 2H, *S-p*-C₆H₄Br), 7.53 (m, 5H, SCH₂C₆H₅), 7.48 (d, ³*J* = 8.4 Hz, 2H, *S-p*-C₆H₄Br), 7.41 (m, 5H, SCH₂C₆H₅), 5.19 (d, ³*J* = 6.0 Hz, 2H, *p*-MeC₆H₄ⁱPr), 5.08 (d, ³*J* = 6.0 Hz, 2H, *p*-MeC₆H₄ⁱPr), 4.90 (d, ³*J* = 6.0 Hz, 2H, *p*-MeC₆H₄ⁱPr), 4.75 (d, ³*J* = 6.0 Hz, 2H, *p*-MeC₆H₄ⁱPr), 3.67 (s, 2H, SCH₂C₆H₅), 3.50 (s, 2H, SCH₂C₆H₅), 1.96 [sept, ³*J* = 6.8 Hz, 2H, *p*-MeC₆H₄CH(CH₃)₂], 1.78 (s, 6H, *p*-CH₃C₆H₄ⁱPr), 1.00 [d, ³*J* = 6.8 Hz, 6H, *p*-MeC₆H₄CH(CH₃)₂], 0.94 [d, ³*J* = 6.8 Hz, 6H, *p*-MeC₆H₄CH(CH₃)₂] ppm. ¹³C{¹H} NMR (100 MHz, CDCl₃): δ = 139.7, 139.6, 137.3, 134.3,

131.9, 129.5, 129.3, 128.8, 128.6, 128.2, 128.1, 122.6, 107.3, 100.0, 84.0, 83.9, 83.8, 82.4, 40.2, 40.0, 31.0, 25.3, 23.1, 22.5, 18.1 ppm.

4.2.6. Data for [9]Cl

Yield: 72.8 mg (82%). $C_{40}H_{46}ClFRu_2S_3 \cdot \frac{1}{4} CH_2Cl_2$ (900.8): calcd. C 53.67, H 5.20; found C 53.32, H 5.41. ESI MS (MeOH): $m/z = 845.5 [M]^+$. 1H NMR (400 MHz, $CDCl_3$): $\delta = 7.74$ (m, 2H, *S-p-C_6H_4F*), 7.38 (m, 10H, $SCH_2C_6H_5$), 6.98 (m, 2H, *S-p-C_6H_4F*), 5.10 (d, $^3J = 6.0$ Hz, 2H, *p-MeC_6H_4^iPr*), 4.99 (d, $^3J = 6.0$ Hz, 2H, *p-MeC_6H_4^iPr*), 4.82 (d, $^3J = 6.0$ Hz, 2H, *p-MeC_6H_4^iPr*), 4.65 (d, $^3J = 6.0$ Hz, 2H, *p-MeC_6H_4^iPr*), 3.58 (s, 2H, $SCH_2C_6H_5$), 3.41 (s, 2H, $SCH_2C_6H_5$), 1.83 [sept, $^3J = 6.8$ Hz, 2H, *p-MeC_6H_4CH(CH_3)_2*], 1.69 (s, 6H, *p-CH_3C_6H_4^iPr*), 0.91 [d, $^3J = 6.8$ Hz, 6H, *p-MeC_6H_4CH(CH_3)_2*], 0.85 [d, $^3J = 6.8$ Hz, 6H, *p-MeC_6H_4CH(CH_3)_2*] ppm. ^{19}F NMR (376 MHz, $CDCl_3$): $\delta = -112.0$ ppm. $^{13}C\{^1H\}$ NMR (100 MHz, $CDCl_3$): $\delta = 164.0$, 161.5, 139.6, 134.5, 133.0, 129.5, 129.3, 128.7, 128.6, 128.2, 128.0, 116.1, 115.9, 107.1, 100.0, 83.9, 83.8, 83.7, 82.3, 40.1, 39.9, 30.8, 23.1, 22.4, 18.0 ppm.

4.2.7. Data for [10]Cl

Yield: 81.1 mg (93%). $C_{42}H_{51}ClRu_2S_3 \cdot \frac{1}{2} CH_2Cl_2$ (932.1): calcd. C 54.76, H 5.62; found C 54.79, H 5.62. ESI MS (MeOH): $m/z = 854.19 [M]^+$. 1H NMR (400 MHz, $CDCl_3$): $\delta = 7.71$ (m, 2H, SC_6H_5), 7.39 (m, 10H, $SCH_2CH_2C_6H_5$), 7.30 (m, 3H, SC_6H_5), 5.2 (m, 8H, *p-MeC_6H_4^iPr*), 3.11 (m, 4H, SCH_2CH_2), 2.93 (m, 2H, SCH_2CH_2), 2.69 (m, 2H, SCH_2CH_2), 2.10 [sept, $^3J = 6.8$ Hz, 2H, *p-MeC_6H_4CH(CH_3)_2*], 1.86 (s, 6H, *p-CH_3C_6H_4^iPr*), 1.07 [m, 12H, *p-MeC_6H_4CH(CH_3)_2*] ppm. $^{13}C\{^1H\}$ NMR (100 MHz, $CDCl_3$): $\delta = 139.8$, 138.3, 132.6, 128.9, 128.8, 128.7, 128.5, 126.9, 107.0, 100.3, 84.4, 84.1, 83.9, 83.2, 41.2, 40.2, 38.8, 38.7, 31.0, 23.3, 22.5, 17.9 ppm.

4.2.8. Data for [11]Cl

Yield: 78.5 mg (86%). $C_{45}H_{57}ClRu_2S_3 \cdot \frac{1}{4} CH_2Cl_2$ (952.95): calcd. C 57.03, H 6.08; found C 57.09, H 6.32. ESI MS (MeOH): $m/z = 897.6 [M + H]^+$. 1H NMR (400 MHz, $CDCl_3$): $\delta = 7.53$ [d, $^3J = 8.4$ Hz, 2H, *S-p-C_6H_4CH(CH_3)_2*], 7.43 (m, 10H, $SCH_2CH_2C_6H_5$), 7.08 [d, $^3J = 8.4$ Hz, 2H, *S-p-C_6H_4CH(CH_3)_2*], 5.16 (d, $^3J = 6.0$ Hz, 2H, *p-MeC_6H_4^iPr*), 5.11 (d, $^3J = 6.0$ Hz, 2H, *p-MeC_6H_4^iPr*), 5.10 (d, $^3J = 6.0$ Hz, 2H, *p-MeC_6H_4^iPr*), 5.06 (d, $^3J = 6.0$ Hz, 2H, *p-MeC_6H_4^iPr*), 3.0 (m, 4H, SCH_2CH_2), 2.82 [sept, $^3J = 6.8$ Hz, 1H, *S-p-C_6H_4CH(CH_3)_2*], 2.78 (m, 2H, SCH_2CH_2), 2.62 (t, $^3J = 7.6$ Hz, 2H, SCH_2CH_2), 1.95 [sept, $^3J = 6.8$ Hz, 2H, *p-MeC_6H_4CH(CH_3)_2*], 1.90 (s, 6H, *p-CH_3C_6H_4^iPr*), 1.29 [d, $^3J = 6.8$ Hz, 6H, *S-p-C_6H_4CH(CH_3)_2*], 1.00 [m, 12H, *p-MeC_6H_4CH(CH_3)_2*] ppm. $^{13}C\{^1H\}$ NMR (100 MHz, $CDCl_3$): $\delta = 149.7$, 132.6, 128.9, 128.8, 127, 106.7, 100.6, 84.1, 83.9, 83.6, 83.4, 33.8, 30.8, 23.9, 23.4, 22.4, 18.0 ppm.

4.2.9. Data for [12]Cl

Yield: 77.8 mg (84%). $C_{46}H_{59}ClRu_2S_3 \cdot \frac{1}{4} CH_2Cl_2$ (966.99): calcd. C 57.45, H 6.20; found C 57.37, H 6.02. ESI MS (MeOH): $m/z = 911.6 [M + H]^+$. 1H NMR (400 MHz, $CDCl_3$): $\delta = 7.54$ [d, $^3J = 8.0$ Hz, 2H, *S-p-C_6H_4C(CH_3)_3*], 7.35 (m, 10H, *S-p-CH_2CH_2C_6H_5*), 7.24 [m, 2H, *S-p-C_6H_4CH(CH_3)_2*], 5.10 (m, 8H, *p-MeC_6H_4^iPr*), 3.04 (m, 2H, SCH_2CH_2), 2.97 (m, 2H, SCH_2CH_2), 2.82 (m, 2H, SCH_2CH_2), 2.58 (m, 2H, SCH_2CH_2), 1.90 [m, 2H, *p-MeC_6H_4CH(CH_3)_2*], 1.80 (s, 6H, *p-CH_3C_6H_4^iPr*), 1.28 [s, 9H, *S-p-C_6H_4C(CH_3)_3*], 0.94 [m, 12H, *p-MeC_6H_4CH(CH_3)_2*] ppm. $^{13}C\{^1H\}$ NMR (100 MHz, $CDCl_3$): $\delta = 151.9$, 139.9, 134.7, 132.2, 128.9, 128.8, 128.7, 126.9, 125.8, 106.5, 100.7, 84.5, 83.9, 83.7, 83.4, 41.2, 40.2, 38.9, 38.8, 34.7, 31.2, 30.7, 23.4, 22.3, 18.0 ppm.

4.2.10. Data for [13]Cl

Yield: 78.1 (88%). $C_{42}H_{51}ClORu_2S_3 \cdot \frac{1}{4} CH_2Cl_2$ (923.83): calcd. C 54.75, H 5.60; found C 54.72, H 5.80. ESI MS (MeOH): $m/z = 870.8 [M + H]^+$. 1H NMR (400 MHz, $CDCl_3$): $\delta = 9.79$ (s, 1H, *S-p-C_6H_4OH*),

7.47 (d, $^3J = 8.8$ Hz, 2H, *S-p-C_6H_4OH*), 7.39 (m, 10H, $SCH_2CH_2C_6H_5$), 7.16 (m, 2H, *S-p-C_6H_4OH*), 5.18 (d, $^3J = 6.0$ Hz, 2H, *p-MeC_6H_4^iPr*), 5.15 (d, $^3J = 6.0$ Hz, 2H, *p-MeC_6H_4^iPr*), 5.11 (d, $^3J = 6.0$ Hz, 2H, *p-MeC_6H_4^iPr*), 5.05 (d, $^3J = 6.0$ Hz, 2H, *p-MeC_6H_4^iPr*), 3.07 (m, 4H, SCH_2CH_2), 2.83 (t, $^3J = 7.6$ Hz, 2H, SCH_2CH_2), 2.66 (t, $^3J = 7.6$ Hz, 2H, SCH_2CH_2), 2.16 [sept, $^3J = 6.8$ Hz, 2H, *p-MeC_6H_4CH(CH_3)_2*], 1.80 (s, 6H, *p-CH_3C_6H_4^iPr*), 1.10 [m, 12H, *p-MeC_6H_4CH(CH_3)_2*] ppm. $^{13}C\{^1H\}$ NMR (100 MHz, $CDCl_3$): $\delta = 159.2$, 139.9, 133.5, 128.8, 128.7, 126.9, 126.8, 125.2, 117.0, 107.1, 100.0, 84.5, 84.0, 83.4, 82.9, 40.4, 40.0, 38.8, 38.7, 30.9, 23.2, 22.7, 17.8 ppm.

4.2.11. Data for [14]Cl

Yield: 80.7 mg (85%). $C_{42}H_{50}BrClRu_2S_3 \cdot \frac{1}{2} CH_2Cl_2$ (1011.01): calcd. C 50.49, H 5.08; found C 50.32, H 5.23. ESI MS (MeOH): $m/z = 932.8 [M]^+$. 1H NMR (400 MHz, $CDCl_3$): $\delta = 7.63$ (d, $^3J = 8.4$ Hz, 2H, *S-p-C_6H_4Br*), 7.40 (m, 10H, $SCH_2CH_2C_6H_5$), 7.34 (m, 2H, *S-p-C_6H_4Br*), 5.21 (m, 8H, *p-MeC_6H_4^iPr*), 3.12 (m, 2H, SCH_2CH_2), 3.06 (m, 2H, SCH_2CH_2), 2.94 (m, 2H, SCH_2CH_2), 2.66 (m, 2H, SCH_2CH_2), 2.10 [sept, $^3J = 6.8$ Hz, 2H, *p-MeC_6H_4CH(CH_3)_2*], 1.85 (s, 6H, *p-CH_3C_6H_4^iPr*), 1.05 [m, 12H, *p-MeC_6H_4CH(CH_3)_2*] ppm. $^{13}C\{^1H\}$ NMR (100 MHz, $CDCl_3$): $\delta = 140$, 139.7, 137.7, 134.2, 131.8, 131.6, 128.7, 128.6, 126.7, 122.4, 107.1, 100.0, 84.1, 83.8, 83.6, 83.0, 41.3, 39.9, 38.7, 38.6, 30.9, 22.8, 17.8 ppm.

4.2.12. Data for [15]Cl

Yield: 80.9 mg (91%). $C_{42}H_{50}ClFRu_2S_3 \cdot \frac{1}{4} CH_2Cl_2$ (928.88): calcd. C 54.63, H 5.48; found C 54.33, H 5.72. ESI MS (MeOH): $m/z = 872.1 [M]^+$. 1H NMR (400 MHz, $CDCl_3$): $\delta = 7.75$ (m, 2H, *S-p-C_6H_4F*), 7.40 (m, 10H, $SCH_2CH_2C_6H_5$), 7.04 (m, 2H, *S-p-C_6H_4F*), 5.24 (m, 8H, *p-MeC_6H_4^iPr*), 3.13 (m, 2H, SCH_2CH_2), 3.09 (m, 2H, SCH_2CH_2), 2.93 (m, 2H, SCH_2CH_2), 2.69 (m, 2H, SCH_2CH_2), 2.13 [sept, $^3J = 6.8$ Hz, 2H, *p-MeC_6H_4CH(CH_3)_2*], 1.87 (s, 6H, *p-CH_3C_6H_4^iPr*), 1.08 [m, 12H, *p-MeC_6H_4CH(CH_3)_2*] ppm. $^{13}C\{^1H\}$ NMR (100 MHz, $CDCl_3$): $\delta = 164.1$, 161.6, 139.8, 134.5, 134.4, 128.9, 128.8, 128.7, 126.9, 116.1, 115.9, 107.1, 100.3, 84.5, 84.3, 83.8, 83.2, 41.4, 40.2, 38.8, 38.7, 31.0, 23.2, 22.5, 18.0 ppm.

4.2.13. Data for [16]Cl

Yield: 78 mg (90%). $C_{48}H_{63}ClRu_2S_3 \cdot \frac{1}{4} CH_2Cl_2$ (995.17): calcd. C 58.24, H 6.43; found C 58.24, H 6.76. ESI MS (MeOH): $m/z = 939.3 [M + H]^+$. 1H NMR (400 MHz, $CDCl_3$): $\delta = 7.76$ (m, 2H, SC_6H_5), 7.47 (m, 4H, *S-p-CH_2C_6H_4^tBu*), 7.42 (m, 4H, *S-p-CH_2C_6H_4^tBu*), 7.32 (m, 3H, SC_6H_5), 5.11 (d, $^3J = 6.0$ Hz, 2H, *p-MeC_6H_4^iPr*), 5.01 (d, $^3J = 6.0$ Hz, 2H, *p-MeC_6H_4^iPr*), 4.91 (d, $^3J = 6.0$ Hz, 2H, *p-MeC_6H_4^iPr*), 4.61 (d, $^3J = 6.0$ Hz, 2H, *p-MeC_6H_4^iPr*), 3.62 (s, 2H, *S-p-CH_2C_6H_4^tBu*), 3.44 (s, 2H, *S-p-CH_2C_6H_4^tBu*), 1.88 [sept, $^3J = 6.8$ Hz, 2H, *p-MeC_6H_4CH(CH_3)_2*], 1.76 (s, 6H, *p-CH_3C_6H_4^iPr*), 1.37 [s, 9H, $SCH_2C_6H_5C(CH_3)_3$], 1.33 [s, 9H, $SCH_2C_6H_5C(CH_3)_3$], 0.93 [d, $^3J = 6.8$ Hz, 6H, *p-MeC_6H_4CH(CH_3)_2*], 0.88 [d, $^3J = 6.8$ Hz, 6H, *p-MeC_6H_4CH(CH_3)_2*] ppm. $^{13}C\{^1H\}$ NMR (100 MHz, $CDCl_3$): $\delta = 151.7$, 151.6, 137.8, 136.7, 132.7, 129.3, 129.2, 129.0, 128.5, 125.6, 125.4, 106.9, 100.4, 84.1, 83.7, 82.4, 40.0, 39.5, 34.8, 34.7, 31.4, 30.8, 23.1, 22.7, 18.2 ppm.

4.2.14. Data for [17]Cl

Yield: 78.6 mg (87%). $C_{51}H_{69}ClRu_2S_3 \cdot 2 CH_3(CH_2)_4CH_3$ (1188.23): calcd. C 63.15, H 8.08; found C 63.41, H 8.32. ESI MS (MeOH + CH_2Cl_2): $m/z = 980.2 [M]^+$. 1H NMR (400 MHz, $CDCl_3$): $\delta = 7.70$ [d, $^3J = 8.4$ Hz, 2H, *S-p-C_6H_4CH^iPr*], 7.50 (m, 4H, *S-p-CH_2C_6H_4^tBu*), 7.46 (m, 4H, *S-p-CH_2C_6H_4^tBu*), 7.20 [d, $^3J = 8.4$ Hz, 2H, *S-p-C_6H_4CH^iPr*], 5.16 (d, $^3J = 6.0$ Hz, 2H, *p-MeC_6H_4^iPr*), 5.03 (d, $^3J = 6.0$ Hz, 2H, *p-MeC_6H_4^iPr*), 4.97 (d, $^3J = 6.0$ Hz, 2H, *p-MeC_6H_4^iPr*), 4.60 (d, $^3J = 6.0$ Hz, 2H, *p-MeC_6H_4^iPr*), 3.65 (s, 2H, *S-p-CH_2C_6H_4^tBu*), 3.47 (s, 2H, *S-p-CH_2C_6H_4^tBu*), 2.95 [sept, $^3J = 6.8$ Hz, 1H, *S-p-C_6H_4CH(CH_3)_2*], 1.85 [sept, $^3J = 6.8$ Hz, 2H,

p-MeC₆H₄CH(CH₃)₂, 1.82 (s, 6H, *p*-CH₃C₆H₄¹Pr), 1.41 [s, 9H, *S*-p-CH₂C₆H₄C(CH₃)₃], 1.37 [s, 9H, *S*-p-CH₂C₆H₄C(CH₃)₃], 1.26 [m, 6H, *S*-p-C₆H₄CH(CH₃)₂], 0.94 [d, ³J = 6.8 Hz, 6H, *p*-MeC₆H₄CH(CH₃)₂], 0.90 [d, ³J = 6.8 Hz, 6H, *p*-MeC₆H₄CH(CH₃)₂] ppm. ¹³C{¹H} NMR (100 MHz, CDCl₃): δ = 151.7, 151.6, 136.8, 136.7, 134.5, 134.4, 132.5, 129.3, 129.1, 127.0, 125.6, 125.4, 106.6, 100.7, 84.6, 83.4, 83.3, 82.5, 34.8, 34.7, 33.8, 31.4, 30.6, 23.9, 23.1, 22.5, 18.2 ppm.

4.2.15. Data for [18]Cl

Yield: 87 mg (95%). C₅₂H₇₁ClRu₂S₃ · 1/8 CH₂Cl₂ (1040.53): calcd. C 60.17, H 6.90; found C 59.03, H 7.02. ESI MS (MeOH): *m/z* = 995.4 [M + H]⁺. ¹H NMR (400 MHz, CDCl₃): δ = 7.66 (d, ³J = 8.4 Hz, 2H, *S*-p-C₆H₄¹Bu), 7.47 (m, 4H, *S*-p-CH₂C₆H₄¹Bu), 7.41 (m, 4H, *S*-p-CH₂C₆H₄¹Bu), 7.32 (d, ³J = 8.4 Hz, 2H, *S*-p-C₆H₄¹Bu), 5.11 (d, ³J = 6.0 Hz, 2H, *p*-MeC₆H₄¹Pr), 4.99 (d, ³J = 6.0 Hz, 2H, *p*-MeC₆H₄¹Pr), 4.95 (d, ³J = 6.0 Hz, 2H, *p*-MeC₆H₄¹Pr), 4.55 (d, ³J = 6.0 Hz, 2H, *p*-MeC₆H₄¹Pr), 3.61 (s, 2H, *S*-p-CH₂C₆H₄¹Bu), 3.42 (s, 2H, *S*-p-CH₂C₆H₄¹Bu), 1.81 [sept, ³J = 6.8 Hz, 2H, *p*-MeC₆H₄CH(CH₃)₂], 1.79 (s, 6H, *p*-CH₃C₆H₄¹Pr), 1.37 [s, 9H, *S*-p-C₆H₄C(CH₃)₃], 1.33 [s, 9H, *S*-p-CH₂C₆H₄C(CH₃)₃], 1.32 [s, 9H, *S*-p-CH₂C₆H₄C(CH₃)₃], 0.89 [d, ³J = 6.8 Hz, 6H, *p*-MeC₆H₄CH(CH₃)₂], 0.86 [d, ³J = 6.8 Hz, 6H, *p*-MeC₆H₄CH(CH₃)₂] ppm. ¹³C{¹H} NMR (100 MHz, CDCl₃): δ = 151.9, 151.7, 151.5, 136.8, 136.7, 134.3, 132.3, 129.3, 129.2, 125.9, 125.7, 125.6, 125.4, 106.4, 100.9, 84.9, 83.3, 83.2, 82.6, 40.1, 39.6, 34.8, 34.7, 31.4, 31.3, 30.6, 23.2, 22.5, 18.3 ppm.

4.2.16. Data for [19]Cl

Yield: 82.8 mg (94%). C₄₈H₆₃ClORu₂S₃ · 1/4 CH₂Cl₂ (1011.02): calcd. C 57.32, H 6.33; found C 57.46, H 6.60. ESI MS (MeOH): *m/z* = 954.9 [M]⁺. ¹H NMR (400 MHz, CDCl₃): δ = 10.33 (s, 1H, *S*-p-C₆H₄OH), 7.50 (m, 2H, *S*-p-C₆H₄OH), 7.48 (m, 8H, *S*-p-CH₂C₆H₄¹Bu), 7.25 (d, ³J = 8.4 Hz, 2H, *S*-p-C₆H₄OH), 5.03 (d, ³J = 6.0 Hz, 2H, *p*-MeC₆H₄¹Pr), 4.93 (d, ³J = 6.0 Hz, 2H, *p*-MeC₆H₄¹Pr), 4.75 (d, ³J = 6.0 Hz, 2H, *p*-MeC₆H₄¹Pr), 4.62 (d, ³J = 6.0 Hz, 2H, *p*-MeC₆H₄¹Pr), 3.58 (s, 2H, *S*-p-CH₂C₆H₄¹Bu), 3.40 (s, 2H, *S*-p-CH₂C₆H₄¹Bu), 2.01 [sept, ³J = 6.8 Hz, 2H, *p*-MeC₆H₄CH(CH₃)₂], 1.73 (s, 6H, *p*-CH₃C₆H₄¹Pr), 1.40 [s, 9H, *S*-p-CH₂C₆H₄C(CH₃)₃], 1.38 [s, 9H, *S*-p-CH₂C₆H₄C(CH₃)₃], 1.02 [d, ³J = 6.8 Hz, 6H, *p*-MeC₆H₄CH(CH₃)₂], 0.97 [d, ³J = 6.8 Hz, 6H, *p*-MeC₆H₄CH(CH₃)₂] ppm. ¹³C{¹H} NMR (100 MHz, CDCl₃): δ = 159.9, 151.8, 151.7, 136.8, 136.6, 133.3, 129.2, 129.0, 125.5, 125.4, 124.1, 117.1, 107.3, 100.1, 83.9, 83.5, 83.4, 82.1, 39.7, 39.0, 34.8, 34.7, 31.4, 30.9, 23.1, 22.8, 18.0 ppm.

4.2.17. Data for [20]Cl

Yield: 77.7 mg (83%). C₄₈H₆₂BrClRu₂S₃ · 1/2 CH₂Cl₂ (1095.15): calcd. C 53.19, H 5.80; found C 52.99, H 5.95. ESI MS (MeOH): *m/z* = 1017.8 [M]⁺. ¹H NMR (400 MHz, CDCl₃): δ = 7.72 (m, 2H, *S*-p-C₆H₄Br), 7.50 (m, 8H, *S*-p-CH₂C₆H₄¹Bu), 7.48 (m, 2H, *S*-p-C₆H₄Br), 5.17 (d, ³J = 6.0 Hz, 2H, *p*-MeC₆H₄¹Pr), 5.08 (d, ³J = 6.0 Hz, 2H, *p*-MeC₆H₄¹Pr), 4.96 (d, ³J = 6.0 Hz, 2H, *p*-MeC₆H₄¹Pr), 4.66 (d, ³J = 6.0 Hz, 2H, *p*-MeC₆H₄¹Pr), 3.64 (s, 2H, *S*-p-CH₂C₆H₄¹Bu), 3.46 (s, 2H, *S*-p-CH₂C₆H₄¹Bu), 1.94 [sept, ³J = 6.8 Hz, 2H, *p*-MeC₆H₄CH(CH₃)₂], 1.79 (s, 6H, *p*-CH₃C₆H₄¹Pr), 1.39 [s, 9H, *S*-p-CH₂C₆H₄C(CH₃)₃], 1.36 [s, 9H, *S*-p-CH₂C₆H₄C(CH₃)₃], 0.97 [d, ³J = 6.8 Hz, 6H, *p*-MeC₆H₄CH(CH₃)₂], 0.92 [d, ³J = 6.8 Hz, 6H, *p*-MeC₆H₄CH(CH₃)₂] ppm. ¹³C{¹H} NMR (100 MHz, CDCl₃): δ = 151.8, 151.6, 137.4, 136.6, 134.2, 131.9, 129.3, 129.1, 125.6, 125.4, 122.6, 107.2, 100.4, 83.9, 83.8, 83.7, 82.4, 40.0, 39.5, 34.8, 34.7, 31.4, 30.9, 23.0, 22.7, 18.2 ppm.

4.2.18. Data for [21]Cl

Yield: 78.5 mg (89%). C₄₈H₆₂ClFRu₂S₃ · 1/3 CH₂Cl₂ (1020.1): calcd. C 57.64, H 6.32; found C 57.43, H 6.74. ESI MS (MeOH): *m/z* = 957.6 [M + H]⁺. ¹H NMR (400 MHz, CDCl₃): δ = 7.75 (m, 2H, *S*-p-C₆H₄F), 7.41 (m, 8H, *S*-p-CH₂C₆H₄¹Bu), 7.00 (m, 2H, *S*-p-C₆H₄F), 5.08 (d, ³J = 6.0 Hz, 2H, *p*-MeC₆H₄¹Pr), 4.99 (d, ³J = 6.0 Hz, 2H, *p*-MeC₆H₄¹Pr),

4.88 (d, ³J = 6.0 Hz, 2H, *p*-MeC₆H₄¹Pr), 4.57 (d, ³J = 6.0 Hz, 2H, *p*-MeC₆H₄¹Pr), 3.56 (s, 2H, *S*-p-CH₂C₆H₄¹Bu), 3.38 (s, 2H, *S*-p-CH₂C₆H₄¹Bu), 1.85 [sept, ³J = 6.8 Hz, 2H, *p*-MeC₆H₄CH(CH₃)₂], 1.71 (s, 6H, *p*-CH₃C₆H₄¹Pr), 1.34 [s, 9H, SCH₂C₆H₄C(CH₃)₃], 1.31 [s, 9H, SCH₂C₆H₄C(CH₃)₃], 0.89 [d, ³J = 6.8 Hz, 6H, *p*-MeC₆H₄CH(CH₃)₂], 0.85 [d, ³J = 6.8 Hz, 6H, *p*-MeC₆H₄CH(CH₃)₂] ppm. ¹³C{¹H} NMR (100 MHz, CDCl₃): δ = 164.1, 161.6, 151.7, 151.6, 134.4, 133.2, 129.2, 129.0, 125.5, 125.4, 116.1, 115.9, 106.9, 100.4, 84.0, 83.7, 83.6, 82.4, 39.9, 39.4, 34.7, 31.4, 30.8, 23.0, 22.6, 18.2 ppm.

4.3. Cell culture and inhibition of cell growth

Human A2780 and A2780cisR ovarian cancer cells were obtained from the European Collection of Cell Cultures (Salisbury, UK). Cells were grown routinely in RPMI-1640 medium supplemented with 10% foetal calf serum (FCS) and antibiotics at 37 °C and 5% CO₂. Cytotoxicity was determined using the MTT assay (MTT = 3-(4,5-dimethyl-2-thiazolyl)-2,5-diphenyl-2H-tetrazolium bromide). Cells were seeded in 96-well plates as monolayers with 100 μL of cell solution (approximately 20 000 cells) per well and pre-incubated for 24 h in medium supplemented with 10% FCS. Compounds were prepared as DMSO solution, then dissolved in the culture medium and serially diluted to the appropriate concentration to give a final DMSO concentration of 0.5%. 100 μL of drug solution was added to each well and the plates were incubated for another 72 h. Subsequently, MTT (5 mg mL⁻¹ solution) was added to the cells and the plates were incubated for a further 2 h. The culture medium was aspirated, and the purple formazan crystals formed by the mitochondrial dehydrogenase activity of vital cells were dissolved in DMSO. The optical density, directly proportional to the number of surviving cells, was quantified at 540 nm using a multiwell plate reader and the fraction of surviving cells was calculated from the absorbance of untreated control cells. Evaluation is based on means from two independent experiments, each comprising three microcultures per concentration level.

4.4. Glutathione oxidation

NMR data were acquired at 37 °C using a Bruker Avance II 500-MHz NMR spectrometer equipped with an inverse dual channel (¹H, X) z-gradient probe head (broadband inverse) or using a Bruker Avance II 400-MHz NMR spectrometer equipped with an inverse dual channel (¹H, X) z-gradient probe head (broadband inverse). One-dimensional ¹H NMR data were acquired with 16–64 transients as 32 768 data points over a width of 12 ppm using a classical presaturation to eliminate the water resonance. A relaxation delay of 6 s was applied between the transients. All NMR data were processed using Topspin (version 2.1 or 3.0, Bruker, Switzerland). The ¹H δ scale was referenced to the residual water signal at 4.637 ppm (37 °C).

To evaluate the catalytic performance of the complexes for the oxidation of the reduced form of GSH to GSSG, the complexes (approximately 0.2 μM) were dissolved in D₂O/DMSO-d₆ (99:1) and 100 equiv of GSH was added to the solution. The samples were subsequently analyzed by ¹H NMR spectroscopy. For the six complexes, the ¹H NMR spectra were recorded immediately after sample preparation, and then every 30 min until complete disappearance of the original resonances of GSH. The TOF₅₀ values were obtained from each catalytic run by fitting the turnover numbers (TON) as a function of time with the exponential expression $Y = a - bc^x$ for all complexes. The turnover numbers were calculated according to the following equation: $\{I_{GSSG}/(I_{GSH} + I_{GSSG})\} \times \{[GSH]_0/[complex]\}$, where I_{GSSG} and I_{GSH} are the integral intensities of the signals of GSSG and GSH respectively. The turnover frequencies were obtained as a derivative of the fitting function for $x = 2$ (after 2 h incubation

corresponding approximately to 50% conversion of GSH to GSSG) and are reported considering only one ruthenium atom.

Acknowledgments

This work was financially supported by the Swiss National Science Foundation (projects no 200020-131844 and 200020-143254) and by the Berne University Research Foundation.

References

- [1] J. Reedijk, *Pure Appl. Chem.* 59 (1987) 181–192.
- [2] E. Wong, C.M. Giandomenico, *Chem. Rev.* 99 (1999) 2451–2466.
- [3] C.G. Hartinger, S. Zorbas-Seifried, M.A. Jakupec, B. Kynast, H. Zorbas, B.K. Keppler, *J. Inorg. Biochem.* 100 (2006) 891–904.
- [4] I. Kostova, *Cur. Med. Chem.* 13 (2006) 1085–1107.
- [5] M.A. Jakupec, E. Reissner, A. Eichinger, M. Pongratz, V.B. Arion, M. Galanski, C.G. Hartinger, B.K. Keppler, *J. Med. Chem.* 48 (2005) 2831–2837.
- [6] M.J. Clarke, *Coord. Chem. Rev.* 236 (2003) 209–232.
- [7] D.R. Frasca, D. Ciampa, J. Emerson, R.S. Umans, M.J. Clarke, *Met. Based Drugs* 3 (1996) 197–209.
- [8] G. Sava, A. Bergamo, S. Zorzet, B. Gava, C. Casarsa, M. Cocchietto, A. Furlani, V. Scarcia, B. Serli, E. Lengo, E. Alessio, G. Mestroni, *Eur. J. Cancer* 38 (2002) 427–435.
- [9] F. Piccioli, S. Sabatini, L. Messori, P. Orioli, C.G. Hartinger, B.K. Keppler, *J. Inorg. Biochem.* 98 (2004) 1135–1142.
- [10] S. Kapitzka, M.A. Jakupec, M. Uhl, B.K. Keppler, B. Marian, *Cancer Lett.* 226 (2005) 115–121.
- [11] C. Scolaro, A. Bergamo, L. Brescacin, R. Delfino, M. Cocchietto, G. Laurency, T.J. Geldbach, G. Sava, P.J. Dyson, *J. Med. Chem.* 48 (2005) 4161–4171.
- [12] M.-G. Mendoza-Ferri, C.G. Hartinger, R.E. Eichinger, N. Stolyarova, K. Severin, M.A. Jakupec, A.A. Nazarov, B.K. Keppler, *Organometallics* 27 (2008) 2405–2407.
- [13] M.-G. Mendoza-Ferri, C.G. Hartinger, A.A. Nazarov, W. Kandioller, K. Severin, B.K. Keppler, *Appl. Organomet. Chem.* 22 (2008) 326–332.
- [14] M. Gras, B. Therrien, G. Süß-Fink, O. Zava, P.J. Dyson, *Dalton Trans.* 39 (2010) 10305–10313.
- [15] F. Giannini, G. Süß-Fink, J. Furrer, *Inorg. Chem.* 50 (2011) 10552–10554.
- [16] F. Giannini, J. Furrer, A.F. Ibaño, G. Süß-Fink, B. Therrien, O. Zava, M. Baquie, P.J. Dyson, P. Štěpnička, *J. Biol. Inorg. Chem.* 17 (2012) 951–960.
- [17] A.F. Ibaño, M. Gras, B. Therrien, G. Süß-Fink, O. Zava, P.J. Dyson, *Eur. J. Inorg. Chem.* 2012 (2012) 1531–1535.
- [18] M.A. Furrer, A. Garci, E. Denoyelle-Di-Muro, P. Trouillas, F. Giannini, J. Furrer, C.M. Clavel, P.J. Dyson, G. Süß-Fink, B. Therrien, *Chem. Eur. J.* 19 (2013) 3198–3203.
- [19] P. Govender, N.C. Antonels, J. Mattsson, A.K. Renfrew, P.J. Dyson, J.R. Moss, B. Therrien, G.S. Smith, *J. Organomet. Chem.* 694 (2009) 3470–3476; (a) P. Govender, A.K. Renfrew, C.M. Clavel, P.J. Dyson, B. Therrien, G.S. Smith, *Dalton Trans.* 40 (2011) 1158.
- [20] C. Hansch, A. Leo, R.W. Taft, *Chem. Rev.* 91 (1991) 165–195.
- [21] Advanced Chemistry Development, ACD/ChemSketch, Version 12.0, Advanced Chemistry Development, Toronto, 2012.
- [22] J. Achrem-Achremowicz, E. Kępczyńska, M. Zylewskib, Z. Janeczko, *Bio-med. Chromatogr.* 24 (2010) 261–267.
- [23] A. Pompella, A. Visvikis, A. Paolicchi, V. De Tata, A.F. Casini, *Biochem. Pharmacol.* 66 (2003) 1499–1503.
- [24] N. Satoh, *Biochem. Genet.* 48 (2010) 816–821.
- [25] A. Pastore, A. Lo Russo, M. Greco, G. Rizzoni, G. Federici, *Clin. Chem.* 47 (2001) 1467–1469.
- [26] C. Scolaro, A.B. Chaplin, C.G. Hartinger, A. Bergamo, M. Cocchietto, B.K. Keppler, G. Sava, P.J. Dyson, *Dalton Trans.* 43 (2007) 5065–5072.
- [27] A.K. Renfrew, L. Juillerat-Jeanneret, P.J. Dyson, *J. Organomet. Chem.* 696 (2011) 772–779.